

# *In Vitro* Performance of Injectable Chitosan-Tripolyphosphate Scaffolds Combined with Platelet-Rich Plasma

Andréa Arruda Martins Shimojo<sup>1</sup>, Sofia Elisa Moraga Galdames<sup>1</sup>, Amanda Gomes Marcelino Perez<sup>1</sup>, Thiago Heiji Ito<sup>2</sup>, Ângela Cristina Malheiros Luzo<sup>3</sup>, Maria Helena Andrade Santana<sup>1\*</sup>

<sup>1</sup>Department of Engineering of Materials and Bioprocesses, School of Chemical Engineering, University of Campinas (UNICAMP), Campinas, Brazil

<sup>2</sup>Department of Physical Chemistry, Institute of Chemistry, University of Campinas (UNICAMP), Campinas, Brazil

<sup>3</sup>Haematology and Hemotherapy Center, Umbilical Cord Blood Bank, University of Campinas (UNICAMP), Campinas, Brazil

This study aimed to evaluate the *in vitro* biological effectiveness of chitosan microparticles crosslinked with sodium tripolyphosphate (TPP) in combination with activated pure platelet-rich plasma (aP-PRP) as an injectable composite scaffold for growth factors release, cell proliferation and osteogenic differentiation. Two main novelties were addressed in the field of scaffolds in regenerative medicine: the first is the approach including simultaneously the three vertices of the proliferation triangle formed by the capabilities genic progenitor cells, conductive scaffolds and inductive growth factors, which are provided by platelet rich plasma (PRP); secondly, the approach of an injectable composite scaffolds formed by the fibrin network from aP-PRP and the chitosan microparticles crosslinked with TPP. The microparticles were prepared by vortexing the chitosan and TPP solutions. The ionic crosslinking of chitosan with TPP was made at mass ratios of 2:1, 5:1, and 10:1 at pH 4.0. P-PRP was obtained via the controlled centrifugation of whole blood. The composite scaffolds were prepared by adding the microparticles to immediately activated P-PRP. The results showed that the microparticles had adequate physico-chemical and mechanical properties for injection. Furthermore, the microparticles controlled the release of growth factors from P-PRP. The proliferation of human adipose-derived mesenchymal stem cells was lower than in aP-PRP alone but significant at a 2:1 chitosan-TPP mass ratio. Osteogenic differentiation was stimulated at all studied mass ratios, as indicated by the alkaline phosphatase activity. These results offer perspectives for optimizing the composite scaffold, and to prove its potential as an injectable scaffold in regenerative medicine.

*Tissue Eng Regen Med* 2016;13(1):21-30

**Key Words:** Chitosan; Tripolyphosphate; Platelet-rich plasma; Injectable scaffolds; Composite

## INTRODUCTION

Due to their minimally invasive implantation procedures, injectable scaffolds have being widely investigated and are considered promising in tissue engineering [1].

From the clinical perspective, the use of injectable scaffolds is advantageous because it minimizes patient discomfort, the risk of infection and scarring, and the cost of treatment [2]. Furthermore, injectable scaffolds can homogeneously fill the defect or

repair point and can incorporate cells and various therapeutic agents such as growth factors prior to injection [3].

From the biomaterial perspective, adequate injectable scaffolds must be nontoxic, biodegradable, and sterilizable. Moreover, they must solidify under mild conditions, show mechanical strength and resistance to in situ forces and allow for the incorporation of bioactive molecules.

Various types of biodegradable materials have been proposed for the preparation of injectable scaffolds used in tissue engineering. Considerable attention has been given to chitosan-based materials, primarily due to their similarities with the extracellular matrix, chemical versatility, good biological performance, and specific cellular interactions [4].

Chitosan scaffolds has been prepared as hydrogels by physical association [5], coordination with metal ions [6] and chemical crosslinking [7]. However, the use of chemical crosslinking

**Received:** December 10, 2014

**Revised:** May 28, 2015

**Accepted:** June 5, 2015

**\*Corresponding author:** Maria Helena Andrade Santana, Department of Engineering of Materials and Bioprocesses, School of Chemical Engineering, University of Campinas (UNICAMP), Albert Einstein, 500, Campinas 13083-852, SP, Brazil.

Tel: 55-19-35213921, Fax: 55-19-35213890

E-mail: mariahelena.santana@gmail.com

agents are a major obstacle to scaffolds due to their toxicity to the cells. Thus, tripolyphosphate (TPP) and genipin have become attractive alternatives to chitosan crosslinking [8-11].

The electrostatic interaction between chitosan and TPP leads to the formation of biocompatible crosslinked chitosan hydrogels, which could be used as injectable scaffolds in micro- and/or nanoparticles in non-surgical treatments.

According to Barnett and Pomeroy [12], tissue regeneration is based on a proliferation triangle composed of cells, bioactive molecules and scaffolds, which are in a close relationship through their capabilities. The scaffolds provide the conductive matrix for supporting the genic capability of progenitor cells mediated by the inductive capability of bioactive molecules. According to Crane and Everts [13], the interaction of each element of this triangle must be present for effective tissue repair and pain relief.

Most of the articles only uses the conductive scaffolds and genic cell capacity, not mimicking the total environment required for cell regeneration. The association with the platelet-rich plasma (PRP) allows not only the release of growth factors and cytokines (inductive capacity) that accelerate the regeneration process, but also its fibrin network acts as a natural scaffold increasing the surface area for cell adhesion, proliferation and differentiation [13-15]. However, the fibrin network is fragile, has low viscosity and viscoelasticity, and undergoes rapid degradation in biological environments. In addition, released growth factors (GFs) have a half-life of only a few hours [16].

Therefore, this article addresses two main novelties in the field of research on scaffolds and regenerative medicine: the first is the approach including simultaneously the three vertices of the proliferation triangle with the capabilities genic, conductive and inductive, which are provided by PRP; secondly the approach of an injectable composite scaffold formed by the fibrin network and the chitosan microparticles crosslinked with TPP, for improvement of stability and controlled release of growth factors.

In our previous studies, we have shown that porous chitosan sponges [17] and porous chitosan sponges stabilized by crosslinking with TPP (unpublished data) had adequate physicochemical properties for tissue engineering uses. Moreover, the sponges associated with activated of pure PRP (aP-PRP), increased the stability of fibrin network, controlled the release of the growth factors [platelet-derived growth factors (PDGF-AB) and transforming growth factor (TGF)- $\beta$ 1] and allowed the proliferation and differentiation of human adipose-derived mesenchymal stem cells (h-AdMSCs).

In the present work, we extended our previous findings by evaluating the performance of the combination of the injectable scaffold composed by chitosan microparticles crosslinked with tripolyphosphate (iCHT-TPPs) and aP-PRP as a compos-

ite scaffold. Our hypothesis is that the microparticles may control the release of growth factors, as well as to stimulate cell proliferation and osteogenic differentiation, with the benefits of an injectable formulation with *in situ* gelation.

## MATERIALS AND METHODS

Chitosan [average molecular weight (Mw)= $4 \times 10^5$  Da, degree of deacetylation= $83 \pm 4\%$ ] was purchased from Polymar<sup>®</sup> company (Fortaleza, Brazil) and purified according to the protocol described by Nasti et al. [18]. Other chemicals were reagent grade and were used without any further purification. All biological experiments were performed with h-AdMSCs and approved by the Ethics Committee of the Medical Sciences School of the University of Campinas (UNICAMP; CAAE: 0972.0.146.000-11). The donors were healthy individuals between 30 and 40 years old and were previously assessed through their clinical examinations.

### Preparation of the microparticles iCHT-TPPs

The injectable scaffolds (iCHT-TPPs) prepared in this work are composed of hydrogels of chitosan microparticles ionically crosslinked with TPP. Purified chitosan was dissolved in acetic acid solution (5/100 mL) to obtain a chitosan concentration of 2.5 g/100 mL and pH of 4.0. Pentasodium TPP was dissolved in water at 5 g/100 mL. The solutions were mixed at mass ratios CHT:TPP of 2:1, 5:1, and 10:1 and vortexed for 5 minutes to obtain the microparticles in a final volume of 30 mL. The mean yields of 3 replicates were calculated by the ratio between weight of swollen microparticles and initial weight of chitosan. The quantitative data were as follows: CHT:TPP 2:1 (15/3.75 mL; yield= $89.0 \pm 0.3\%$ ), 5:1 (15/1.5 mL, yield= $75.6 \pm 0.5\%$ ), and 10:1 (15/0.75 mL; yield= $46.8 \pm 0.8\%$ ).

### Physicochemical characterization

#### Chemical modification

The ionic crosslinking was characterized by Fourier-transform infrared (FTIR) in a Thermo Scientific Nicolet model 6700 (Thermo Scientific Nicolet<sup>™</sup>, Waltham, MA, USA). Measurements were made in the ATR mode with accessory SMART OMNI-SAMPLER, in the spectral range of 4000–675  $\text{cm}^{-1}$  resolution of 4  $\text{cm}^{-1}$  and 64 scans. Pure chitosan was used as a control.

ATR-IR (chitosan): 3500–3000 ( $\nu$  OH and  $\text{NH}_2$ ), 2875 ( $\nu$ CH), 1645 (amide I), 1550 (amide II), 1380 ( $\delta$ C-H), 1067 and 1020 ( $\nu$ asC-O-C and  $\nu$ sC-O-C)  $\text{cm}^{-1}$  [18].

#### Crosslink density Flory-Rehner calculations

Crosslink density was evaluated by measuring the volumet-

ric swelling and using a simplified version of the Flory and Rehner [19] equation, according to Collins and Birkinshaw [20]. The value used for chitosan-water interaction parameter ( $\chi$ ) was 0.5917 [21].

### Charge ratios calculations

The charge ratios ( $R_{+/-}$ ) were estimated using the mass ratios CHT-TPP of microparticles according to modified model of Rädler et al. (equation 1) [22]

$$R_{+/-} = \left[ \frac{f(\text{CHT}^+) \times M(\text{CHT}^+)}{MW(\text{CHT}^+)} \right] \left[ \frac{MW(\text{TPP}^-)}{5 M(\text{TPP}^-)} \right] \quad (1)$$

were,  $R_{+/-}$ ;  $M(\text{CHT}^+)$ ,  $M(\text{TPP}^-)$ ,  $MW(\text{CHT}^+)$ ,  $MW(\text{TPP}^-)$ , and  $f(\text{CHT}^+)$  are respectively the charge ratio between chitosan and TPP; weight of chitosan in g; weight of TPP in g; molecular weight of chitosan and TPP; and the degree of deacetylation of chitosan. The value  $R_{+/-}=1$  corresponds to the stoichiometric charge neutrality.

### Particle diameter measurements

The mean diameter of the particles was evaluated by laser light scattering in a Mastersizer S particle size analyzer, model Long Bench-MAM 5005 (Malvern Instruments, Worcestershire, UK). The particle size analysis was performed with the hydrogels dispersed in water. The standard deviation (SD) was calculated from ten measurements of the mean diameter.

### Rheology measurements

Rheological measurements were performed in steady and oscillatory regimes at 25°C, using a parallel plate geometry of 20 mm. Steady shear measurements were obtained at shear rates of 0.1–50 s<sup>-1</sup>. Oscillatory measurements were conducted in the linear region, at a stress of 1.188 Pa and in the frequency range of 0.01 to 10 Hz. All rheological measurements were performed on a rheometer Haake RheoStress 1 (Haake, Karlsruhe, Germany).

### Extrusion force

Initially the iCHT-TPPs were loaded in 1-mL plastic syringes with 30-gauge needles. Subsequently, the force required to extrude was measured using a MTS 810 Servo-hydraulic Universal Testing Machine (MTS Systems Corporation, Eden Prairie, MN, USA) (Load Cell 1.5 kN) at 25°C at a 5.0 mm/min extrusion rate.

### Swelling ratio

The microparticles were weighed after swelling in phosphate buffered saline (PBS) at pH 7.4, and their dry weight was determined by drying under vacuum (1 mm Hg) at 25°C after 3 days, swelling ratio (SR) was calculated using the equation 2:

$$SR = \frac{w_s}{w_d} \quad (2)$$

where  $w_s$  and  $w_d$  are the weights of the scaffolds at the swelling state and the dry state, respectively.

### Degradation in phosphate buffered saline

The degradation of iCHT-TPPs was examined with respect to weight loss. The weight loss of the initially weighed iCHT-TPPs ( $w_0$ ) was monitored as a function of incubation time in PBS at 37°C. At specified time intervals, iCHT-TPPs were removed from the PBS and weighed ( $w_t$ ). The weight loss ratio was defined as in equation 3 [23].

$$\text{Weight loss (\%)} = \frac{w_0 - w_t}{w_0} \times 100 \quad (3)$$

### Biological characterization

#### Cytotoxicity assay

The cytotoxicity of the iCHT-TPPs was carried out by exposure to h-AdMSCs and cultivation at 37°C for 24 hours. The cytotoxicity was evaluated using a modified MTT [3-(4,5-dimethyl-thiazol-2-yl)-2,5-diphenyltetrazolium bromide] assay (MTT, Molecular Probes®, São Paulo, Brazil) [24]. The MTT assay is a colorimetric test that is based on the reduction of yellow tetrazolium salt into a purple formazan product in presence of cells [25]. Briefly, the cells at the 4 passage were cultivated in Dulbecco's modified Eagle's medium (DMEM, Gibco, Grand Island, NY, USA) supplemented with 10% fetal bovine serum (FBS, Gibco, Grand Island, NY, USA) and 1% penicillin/streptomycin (Gibco, Grand Island, NY, USA) at 37°C in an atmosphere with 5% CO<sub>2</sub> until the time of the cell viability assay. Extracts of the iCHT-TPPs were obtained by incubating in DMEM containing 10% FBS at a proportion of 0.2 g/mL of medium for 48 h at 5% CO<sub>2</sub> and 37°C. Cell suspensions (1 × 10<sup>4</sup> cells/mL) were inoculated into a 96-well cell culture plate (n=3) and cultured with DMEM with 10% FBS at 37°C for 24 h. After this, the medium was replaced by the extract obtained from the iCHT-TPPs and the cells were maintained under these conditions for 24 h. DMEM with phenol 0.5% was used as the positive toxicity control (PTC) and DMEM with 10% FBS as the negative toxicity control (NTC). After incubation time, the medium was removed and the wells were washed with 200 μL PBS and 200 μL pure DMEM. Next, 200 μL of MTT solution in culture medium (0.5 mg MTT/mL) were added, and the plate was incubated in the dark for 4 h at 37°C. The medium with MTT was removed and 200 μL of dimethyl sulfoxide (DMSO, Sigma Aldrich, St. Louis, MO, USA) was added and absorbance was determined at 595 nm (FilterMax F5 Multi-Mode Microplate reader, Molecular Devices, Sunny-

vale, CA, USA).

### Preparation of pure platelet-rich plasma

P-PRP, a PRP type that is rich in platelets and low in leukocytes, was prepared according to Perez et al. [26]. Briefly, whole blood (WB) was collected into 3.5 mL vacuum tubes (Vacuette<sup>®</sup>, Campinas, Brazil) containing sodium citrate 3.2% (w/v) as an anticoagulant. WB was initially centrifuged in a Rotina 380R centrifuge (Hettich<sup>®</sup> Zentrifugen, Tuttlingen, Germany) at 100×g for 10 minutes at 25°C. After the formation of three layers [a bottom layer composed primarily of red blood cells (RBCs); an upper layer composed of plasma, platelets and some white blood cells (WBCs); and an intermediate layer, or buffy coat, composed primarily of WBCs], only the upper layer was collected to obtain P-PRP. The concentrations of platelets, WBCs and RBCs in WB and P-PRP were determined using the ABX Micros ES 60 hematology analyzer (HORIBA ABX Diagnostics, Montpellier, France).

### Activation of P-PRP

aP-PRP was prepared via the activation of P-PRP with autologous serum (Ser) and 10% (w/v) CaCl<sub>2</sub> solution as agonists using the following proportions: agonist/P-PRP=20%; Ser/CaCl<sub>2</sub> volumetric ratio=9. Autologous serum was prepared by collecting 5 mL of WB in tubes without anticoagulant. After 30 minutes of clot formation, WB was centrifuged at 2000×g for 10 minutes [26].

### Preparation of composite scaffold (aP-PRP-iCHT-TPPs)

aP-PRP-iCHT-TPPs was prepared by embedding by dripping aP-PRP, immediately after activation, into iCHT-TPPs. The preparation was carried out in 48-well microplates using 200 µL of aP-PRP/100–200 mg of iCHT-TPPs.

### Characterization of aP-PRP/iCHT-TPPs

#### Release of GFs

The release of PDGF-AB and TGF-β1 was performed after a 1-hour gelation of aP-PRP associated to iCHT-TPPs in the presence of the culture medium DMEM with low glucose concentration (DMEM-LG, Gibco, Grand Island, NY, USA). The culture medium (1.5 mL) was added to aP-PRP/iCHT-TPPs in 48-well microplates, which were maintained in an incubator with 5% CO<sub>2</sub> throughout the assays. The total volume of culture medium was withdrawn at 3, 6, 12, 24, and 72 hours, and the same volume of fresh medium was replaced without removing the hydrogels from the wells. The samples were stored at -80°C for further characterization. The concentrations of the released GFs PDGF-AB and TGF-β1 were measured using enzyme-linked immunosorbent assay kits (R&D Systems, Minneapolis, MN, USA) ac-

ording to the manufacturer's instructions and specifications.

### h-AdMSCs isolation and pre-cultivation

Human subcutaneous adipose tissue acquired from liposuction surgery, were provided and characterized by the Umbilical Cord Blood Bank of the University of Campinas, Brazil. Briefly, the tissue was washed with sterile PBS, separated into fractions of 10 g, digested with 20 mg of collagenase type 1A and maintained in 20 mL of DMEM-LG containing 10% bovine serum albumin and 10 µL of gentamicin for 30 min in a bath at 37°C. After complete digestion, the reaction was quenched with 10 mL FBS and immediately centrifuged for 15 min at 1500 rpm. The supernatant was discarded, and the pellet was suspended in 10 mL DMEM-LG with 10% FBS. After pre-cultivation for 24 h, the culture medium was changed every 3 days; after the fourth passage, the cells were characterized by immunophenotyping using flow cytometry and by adipogenic, osteogenic and chondrogenic differentiation (data not shown) and were then used in the subsequent experiments. The cells were evaluated by the presence of CD29<sup>+</sup>, CD73<sup>+</sup>, CD90<sup>+</sup>, CD105<sup>+</sup>, and HLA-ABC<sup>+</sup> or absence of HLA-DR<sup>+</sup>, and CD34<sup>+</sup>, CD45<sup>+</sup>.

### Culture of human adipose-derived mesenchymal stem cells-seeding in the composite scaffolds

The pre-cultured h-AdMSCs were trypsinized and resuspended in P-PRP to a final cell concentration of 1×10<sup>4</sup> cells/mL. P-PRP containing h-AdMSCs was activated and immediately embedded into the iCHT-TPPs in a 24-well tissue culture plate, using 200 µL of h-AdMSCs+aP-PRP/100–200 mg of iCHT-TPPs. The composite scaffolds with h-AdMSCs were kept at room temperature for 45 minutes for the consolidation of the fibrin network. Activated PRP was used as a control.

### h-AdMSCs proliferation

The cultivation of h-AdMSCs was carried out in 24-well tissue culture plates by adding 1 mL of the culture medium DMEM to the seeded composite scaffolds (n=4). The seeded composite scaffolds was maintained at 37°C along 10 days. Cell proliferation was quantified using the thiazolyl blue tetrazolium bromide (MTT) assay. At cultivation days 3, 5, 7, and 10, the composite scaffolds were removed and transferred to 24-well plates. MTT (1 mL of 1 mg/mL) was then added, and the cultivation proceeded at 37°C for 4 hours. The MTT solution was then discarded, and 1 mL of DMSO was added to dissolve the purple formazan crystals. The samples were shaken at 120 rpm for 30 min to ensure the homogeneous dissolution of the formazan dye, and 200 µL of each sample was then transferred to a 96-well plate. Optical density was measured at 595 nm using a microplate reader (Filter-Max F5 Multi-Mode Microplate reader, Molecular Devices,

Sunnyvale, CA, USA).

### Images of the cell-seeded composite scaffolds

The images of cell-seeded composite scaffolds were obtained by scanning electron microscopy after 5 days of h-AdMSCs proliferation. The cell-seeded composite scaffolds were fixed in a solution of 4% paraformaldehyde and 2.5% glutaraldehyde in phosphate buffer, pH 7.4, for 2 hours. The samples were then dehydrated in ethanol for 15 min intervals in aqueous 50%, 70%, 95%, and 100% ethanol solutions (2×) and dried using the critical point dryer BAL-TEC CPD 030 (BAL-TEC®, Schalksmühle, Germany). After gold coating in Sputter Coater POLARON SC7620 (VG Microtech, Ringmer, UK), the cell-seeded composite scaffolds were visualized using a scanning electron microscope Leo440i (LEO Electron Microscopy/Oxford, Cambridge, UK) with an accelerating voltage of 20 kV.

### Induction of osteogenic differentiation

h-AdMSCs-seeding composite scaffolds were induced to differentiate into the osteogenic lineage by providing the osteogenic medium containing DMEM-LG supplemented with 10% FBS, 1% β-glycerol-phosphate (Sigma-Aldrich, St. Louis, MO, USA), 1% L-ascorbic acid (Sigma-Aldrich, St. Louis, MO, USA), 1% dexamethasone (Sigma-Aldrich, St. Louis, MO, USA) and 1% Penicillin/Streptomycin solution (Gibco, Grand Island, NY, USA). The medium was changed every 7 days.

### Alkaline phosphatase activity

The alkaline phosphatase (ALP) activity produced by h-AdMSCs was determined on day 14. Here, 200 μL of the supernatant was collected and mixed with 200 μL of p-Nitrophenyl phosphate (SIGMAFAST™ p-Nitrophenyl phosphate Tablets, Sigma, St. Louis, MI, USA) as substrate and subsequently incubated at room temperature for 30 minutes. Absorbance was read

immediately on a spectrophotometer at 405 nm.

### Statistical analysis

Each experiment was carried out in triplicate unless otherwise specified. All results are presented as the mean±SD. The experimental data from all of the studies were analyzed using analysis of variance. Statistical significance was set at a *p*-value≤0.05.

## RESULTS

### Crosslinking in the iCHT-TPPs

The ionic crosslinking in iCHT-TPPs was characterized by FTIR by the presence of the P=O group at the frequencies of 1100 cm<sup>-1</sup> and 1232 cm<sup>-1</sup> and P-O-P asymmetric stretching at 892 cm<sup>-1</sup>. Pure chitosan was used as control.

The FTIR spectra of pure chitosan and iCHT-TPPs 2:1 are shown in Figure 1.

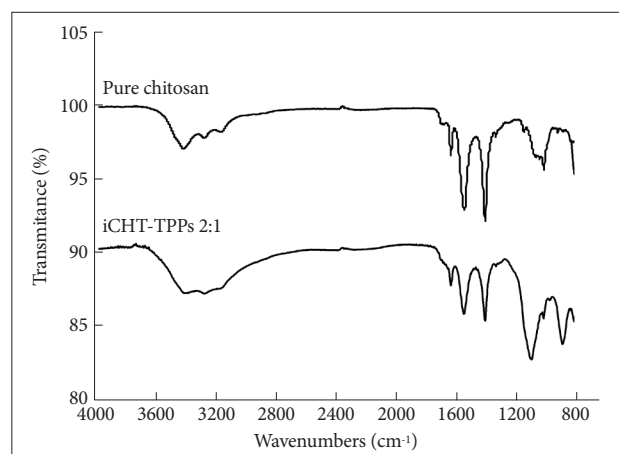


**Figure 1.** FTIR spectra of pure chitosan and iCHT-TPPs 2:1. FTIR: Fourier-transform infrared, iCHT-TPPs: injectable scaffold of chitosan microparticles crosslinked with tripolyphosphate.

**Table 1.** Physicochemical and mechanical properties of iCHT-TPPs

		Physicochemical properties			
Mass ratio (iCHT-TPPs)	SR*	V <sub>c</sub> (mol.cm <sup>-3</sup> )	M <sub>c</sub> (g.mol <sup>-1</sup> )	R <sub>+/·</sub>	Particle diameter (μm)*
2:1	22±1	2.4×10 <sup>-4</sup>	5110	0.7	152±4
5:1	31±1	1.3×10 <sup>-4</sup>	9450	1.8	205±3
10:1	44±1	7.5×10 <sup>-5</sup>	16669	3.6	215±4
		Rheological properties			
Mass ratio (iCHT-TPPs)	G' in 1 Hz (Pa)	n	tan δ	Extrusion force (n)†	
2:1	522	0.04	0.134	12.6±0.9	
5:1	333	0.15	0.174	10.8±0.4	
10:1	72	0.32	0.276	11.1±0.8	

\*the means difference is significant at the 0.05 level, †the means difference is not significant at the 0.05 level. SR: swelling ratio, V<sub>c</sub>: effective crosslink density, M<sub>c</sub>: molecular weight between crosslinks, R<sub>+/·</sub>: charge ratio, G': elastic moduli, G'': viscous moduli, tan δ: G''/G'; n: flow behavior index, iCHT-TPPs: injectable scaffolds of chitosan microparticles crosslinked with TPP



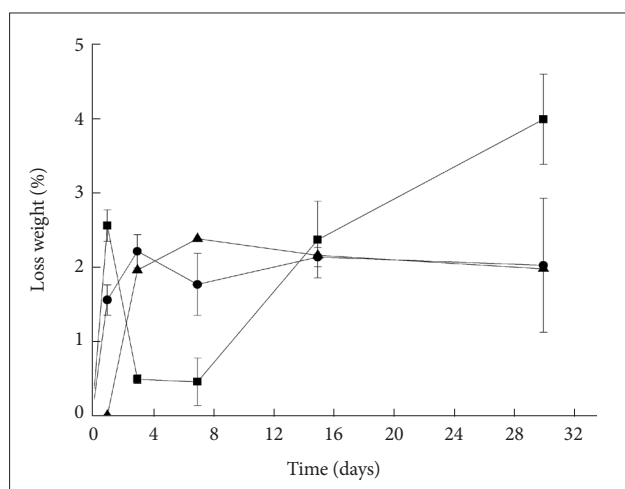
## Physicochemical and mechanical properties of iCHT-TPPs

Table 1 shows the physicochemical and mechanical properties of iCHT-TPPs prepared by varying the CHT-TPP mass ratio.

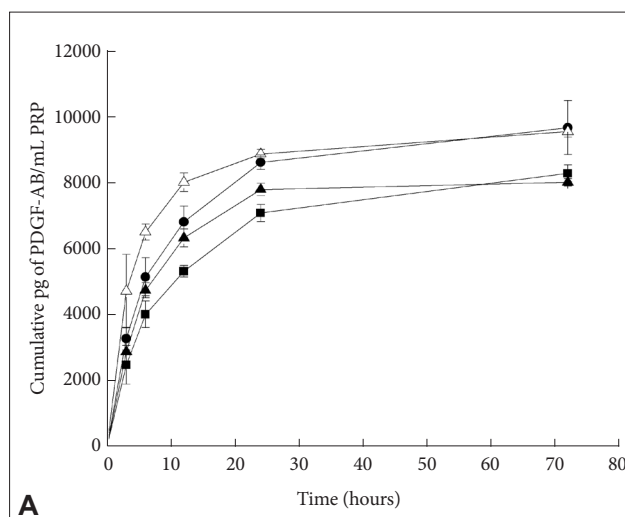
The degradation profile, expressed as the loss weight of iCHT-TPPs after incubation in PBS (pH 7.4, at 37°C) as a function of time, is shown in Figure 2.

## Biological characterization

Figure 3 shows the PDGF-AB and TGF- $\beta$ 1 release kinetics



**Figure 2.** Degradation profile of iCHT-TPPs in PBS pH 7.4 at 37°C. (■) iCHT-TPPs 2:1; (●) iCHT-TPPs 5:1, and (▲) iCHT-TPPs 10:1. iCHT-TPPs: injectable scaffolds of chitosan microparticles crosslinked with TPP, PBS: phosphate buffered saline.



from aP-PRP/iCHT-TPPs.

The micrographs obtained by scanning electronic microscopy of aP-PRP are shown in Figure 4.

Figure 5A shows the proliferation of h-AdMSCs cultured in the presence of iCHT-TPPs, as assayed by MTT. DMEM with phenol 0.5% and DMEM with 10% fetal bovine serum were used as the positive control (PTC) and the negative control (NTC), respectively.

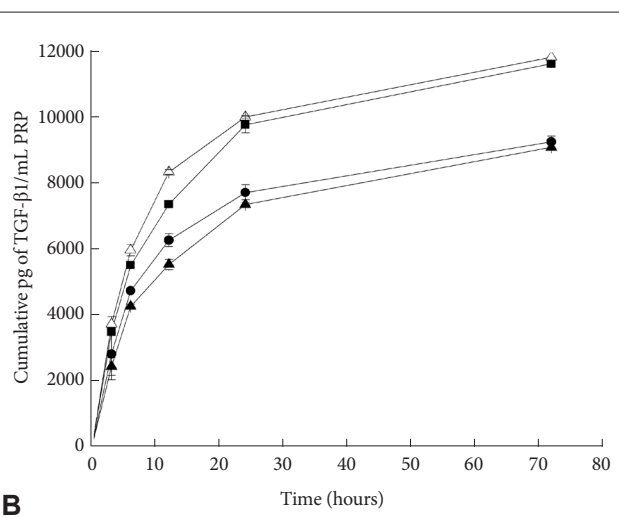
The proliferation profile of h-AdMSCs cultured in aP-PRP/iCHT-TPPs scaffolds as a function of time is shown in Figure 5B. Activated P-PRP was used as control.

Figure 6 shows the results of osteogenic differentiation of h-AdMSCs in the composite scaffolds (aP-PRP-iCHT-TPPs), as assayed by ALP activity.

## DISCUSSION

According to Bhumkar and Pokharkar [8], chitosan (pKa 6.3) may be crosslinked with TPP (pKa 9.7) by two different pH-dependent mechanisms. The ionic crosslinking occurs at low pH values by a reaction between  $\text{NH}_3^+$  groups of chitosan and  $\text{P}_3\text{O}_{10}^{5-}$  of TPP. The deprotonation mechanism occurs at high pH values using the  $\text{OH}^-$  groups of TPP that are present in solution. In this work, the pH of the reaction mixture was maintained at pH 4, which favored the ionic crosslinking mechanism.

The ionic crosslinking between the  $-\text{NH}_3^+$  group of chitosan and  $\text{P}_3\text{O}_{10}^{5-}$  of TPP in iCHT-TPPs was characterized by FTIR (Fig. 1) by the presence of the P=O group at the frequencies of



**Figure 3.** Growth factor release profiles from aP-PRP combined with iCHT-TPPs scaffolds. (A) PDGF-AB and (B) TGF- $\beta$ 1. ( $\Delta$ ) PRP activated with  $\text{Ca}^{2+}$ /serum used as control; (■) aP-PRP/iCHT-TPPs 2:1; (●) aP-PRP/iCHT-TPPs 5:1 and (▲) aP-PRP-iCHT-TPPs 10:1. The concentration of platelets in whole blood donors (average of 2 donors) was  $234250 \text{ pq/mm}^3$ . After preparation of the P-PRP, the platelets were concentrated approximately 2.09 times, with an average final concentration of  $472250 \text{ pq/mm}^3$ . TGF- $\beta$ 1: transforming growth factor  $\beta$ 1, PRP: platelet-rich plasma, aP-PRP: activated pure PRP, iCHT-TPPs: injectable scaffolds of chitosan microparticles crosslinked with TPP, PDGF-AB: platelet-derived growth factor AB, aP-PRP-iCHT-TPPs: injectable scaffolds of chitosan-sodium tripolyphosphates composite scaffold of iCHT-TPPs and aP-PRP, TPP: tripolyphosphate.

1100  $\text{cm}^{-1}$  and 1232  $\text{cm}^{-1}$  and P-O-P asymmetric stretching at 892  $\text{cm}^{-1}$ , according to Mi et al. [27].

The physicochemical properties (Table 1) of chitosan microparticles crosslinked with sodium tripolyphosphate (TPP) were characterized by swelling ratio (SR), effective crosslink density ( $V_e$ ), molecular weight between crosslinks ( $M_c$ ), charge ratio ( $R_{+/-}$ ) and particle diameter.

The water absorption capacity (swelling properties) of scaffolds must be carefully controlled to allow handling during cell implantation and promote cell growth. When hydrated, the scaffolds became fragile being deformed and/or broken with the application of weak forces. Thus, a balance between the viscoelastic and swelling properties is essential to maintain the integrity of scaffolds and support the cell proliferation and differentiation.

The iCMT-TPPs showed a high SR (Table 1), allowing for fast hydration when culture medium was added. Moreover, the microparticles showed a statistically significant increase ( $p <$

0.05) with the degree of crosslinking because of the decreased availability of functional groups to hydrogen bonds with water.

Flory and Rehner [19] calculations were used to determine  $V_e$  and  $M_c$ . The decrease of the CHT-TPP mass ratio increased  $V_e$ , as expected. Moreover, we observed lower  $M_c$  values, indicating higher entanglement of chains.

$R_{+/-}$  of iCMT-TPPs was estimated according to Rädler et al. [22]. The values of  $R_{+/-}$  were negative for iCMT-TPPs 2:1 and positive for iCMT-TPPs 5:1 and 10:1. Therefore, the increase in the crosslinking degree decreased the positive charge of chitosan in the complex. These modifications to the charge ratio may change the interactions with the fibrin network and alter the electrostatic interaction with growth factors.

iCMT-TPPs had a mean diameter in the range of 150 to 220  $\mu\text{m}$ , which was proportional to the CHT-TPP mass ratio. These diameters are within the adequate range for an injectable application ( $<700 \mu\text{m}$ ) [28].

The mechanical properties (Table 1), rheological properties,

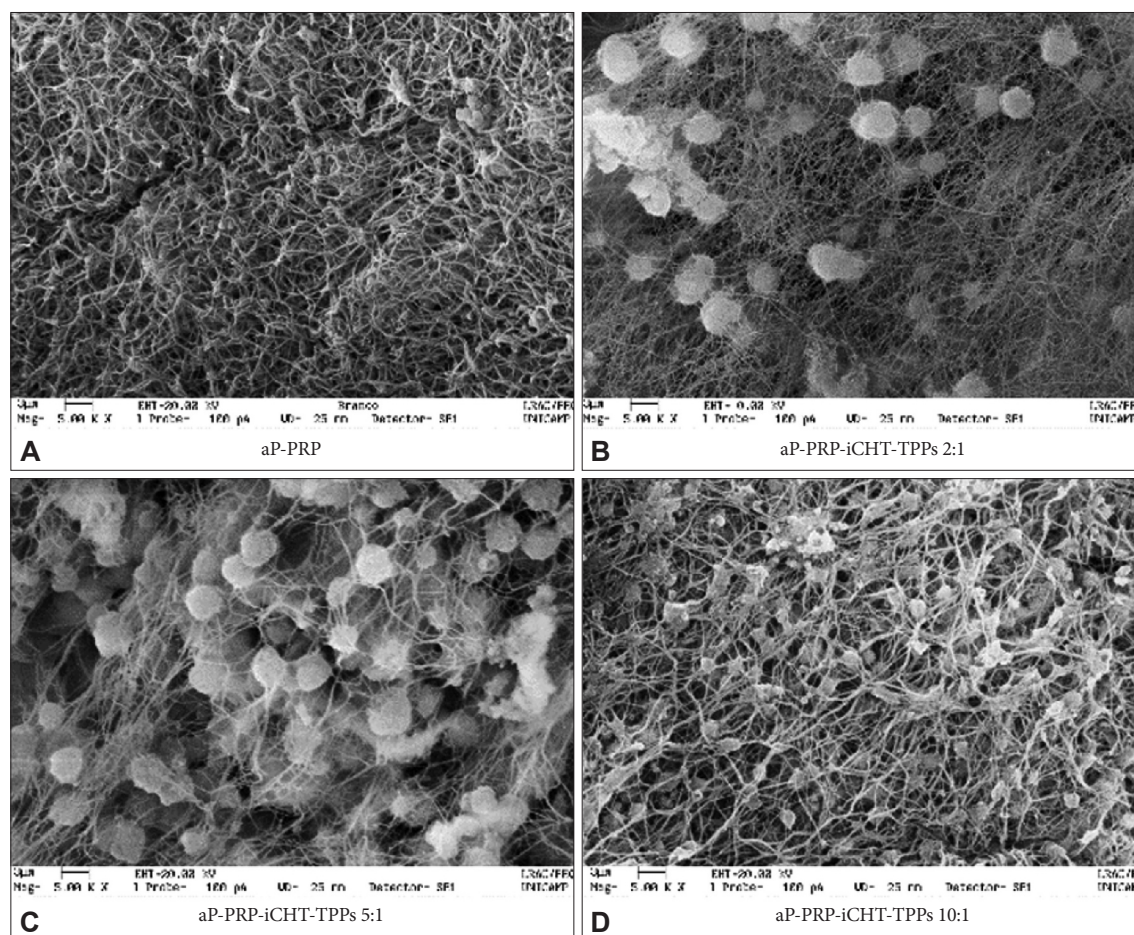


**Figure 4.** Scanning electron microscopic images of aP-PRP and aP-PRP/iCMT-TPPs after 5 days of cultivation of h-AdMSCs. (A) aP-PRP. (B) aP-PRP-iCMT-TPPs 2:1. (C) aP-PRP-iCMT-TPPs 5:1. (D) aP-PRP-iCMT-TPPs 10:1. Scale bar: 3  $\mu\text{m}$ , magnification:  $\times 5000$ . aP-PRP: activated pure platelet-rich plasma, iCMT-TPPs: injectable scaffolds of chitosan microparticles crosslinked with tripolyphosphate, h-AdMSCs: human adipose-derived mesenchymal stem cells.

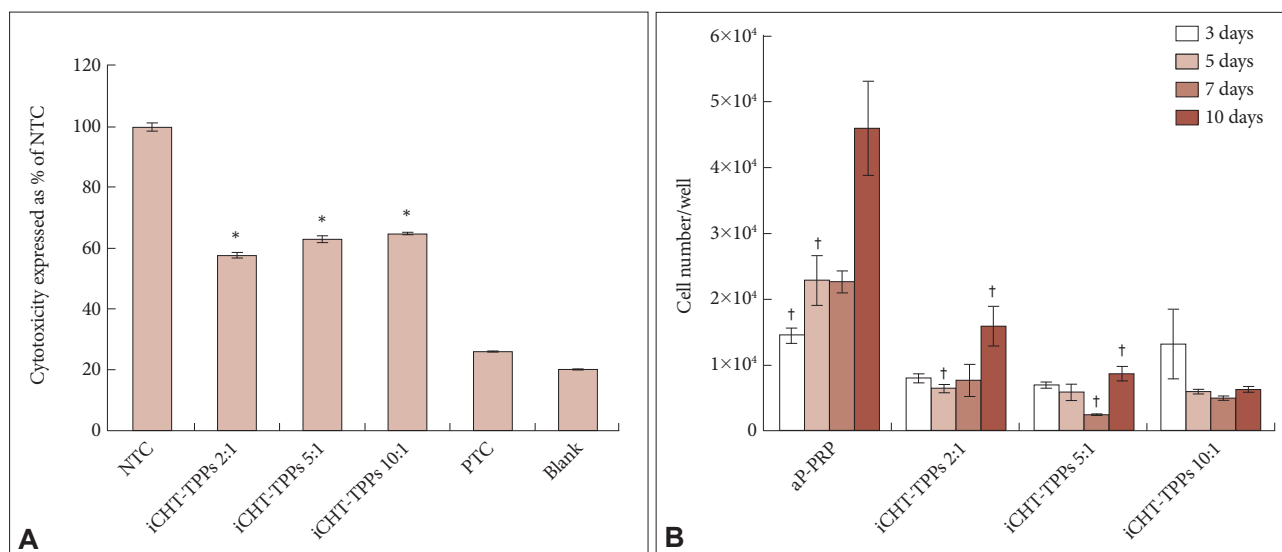


**Figure 5.** (A) % of NTC as a measurement of the cytotoxicity of h-AdMSCs that were exposed to the iCHT-TPPs. Negative (non-toxic) toxicity control (NTC)=DMEM with 10% fetal bovine serum; positive (toxic) toxicity control (PTC)=DMEM with phenol 0.5%. \*the population means (n=3) are significantly different from PTC and NTC at  $p < 0.05$ . (B) Proliferation profile of h-AdMSCs cultured in aP-PRP/iCHT-TPPs scaffolds as a function of time. Activated P-PRP was used as control. Mean  $\pm$  standard deviation (n=3). †The means difference are significantly different at  $p < 0.05$ . h-AdMSCs: human adipose-derived mesenchymal stem cells, iCHT-TPPs: injectable scaffolds of chitosan microparticles crosslinked with TPP, aP-PRP: activated pure platelet rich plasma, TPP: tripolyphosphate.

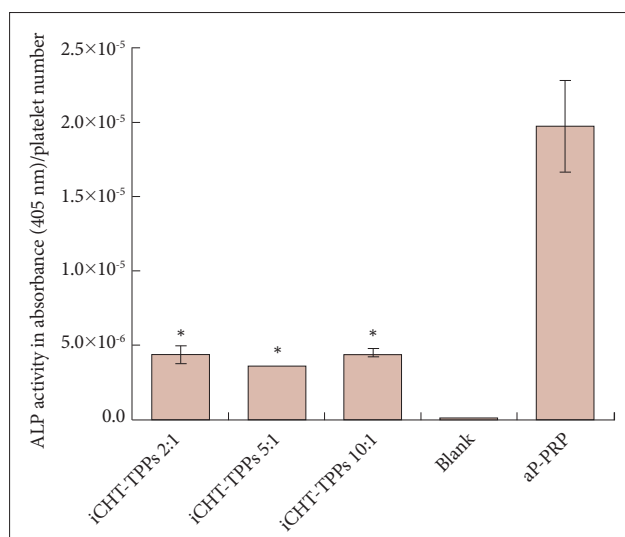


**Figure 6.** ALP activities of h-AdMSCs/platelet number cultured on composite scaffolds. aP-PRP and the reagents used in the assay (blank) were used as control. Mean  $\pm$  standard deviation (n=3). \*the means are significantly different from the controls at 0.05 level. ALP: alkaline phosphatase, h-AdMSCs: human adipose-derived mesenchymal stem cells, iCHT-TPPs: injectable scaffolds of chitosan microparticles crosslinked with TPP, aP-PRP: activated pure platelet-rich plasma, TPP: tripolyphosphate.

extrusion force and degradation profile of the microparticles, were also characterized.

The rheological data show that the iCHT-TPPs exhibited behavior that is typical of so-called weak gels, irrespective of their mass ratios, as analyzed by the storage ( $G'$ ) and loss moduli ( $G''$ ). The moduli had low frequency dependence, and  $\tan$

$\delta > 0.1$  [29,30].

We also observed an increase in the  $G'$  values with the number of crosslinks or entanglements (high  $V_e$  and low  $M_c$ ), which indicated stiffer gels.

In addition, the values of  $\tan \delta$  indicated an increment in gel strength with an increase in  $V_e$ . Regardless of the CHT-TPP mass ratio, iCHT-TPPs showed  $G'$  values that are adequate ( $< 700$  Pa) for injectable application [28].

Considering the Ostwald de Waele power law ( $\eta = K \cdot \dot{\gamma}^{n-1}$ ), the flow behavior index ( $n$ ) of iCHT-TPPs showed a viscoelastic behavior that was dependent on mass ratio. The pseudoplastic behavior is an important parameter in injectable applications, where the flow viscosity should be lower than the rest viscosity.

In addition to the beneficial rheological properties and microparticle size, the injectable scaffolds must have an extrusion force to allow for their easy injection through an appropriately sized needle and thereby prevent side effects such as pain [28].

In iCHT-TPPs, we measured extrusion forces between 10 and 12 N, which were adequate ( $< 20$  N) for injectable applications [31,32]. No significant modification ( $p < 0.05$ ) was observed in the extrusion force with the degree of crosslinking, particle size and distribution, as reported by Bentkover [33].

The degradation profiles (Fig. 2) showed that the microparticles can be considered stable for 30 days, irrespective of the CHT-TPP mass ratio. The maximum loss weight was approximately 4%, for CHT-TPP 2:1.

According to Peppas and Sahlin [34], hydrogels are macro-



molecular networks swollen in water or biological fluids. Hydrogels are often divided into three classes depending on the nature of their network, namely entangled networks, covalently crosslinked networks and networks formed by physical interactions. Physical hydrogels are formed by various reversible links such as association, aggregation, crystallization, complexation, and hydrogen bonding. Most important factors that trigger a physical hydrogel response are pH, temperature and swelling medium.

As the degradation profile is evaluated gravimetrically by weight loss in PBS (pH=7.4) and the chitosan is insoluble in this pH, the degradation in terms of weight lost should be small, as found.

The degradation compete with swelling process and can justify the profiles observed and the values around 4% obtained.

Although there is no statistically significant difference between the degradation profiles, we observed that for iC-HT-TPPs prepared in mass ratios 5:1 and 10:1, the higher weight loss occurred in the first 48 hours whereas for the mass ratio of 2:1, even after 30 days continued to lose mass.

Moreover, as the degradation is directly related to release of growth factors, the low degradation found for iC-HT-TPPs should favor the controlled release of PRP growth factors.

The biological performance of composite scaffolds (aP-PRP-iC-HT-TPPs) was characterized by the release kinetics of growth factors (PDGF-AB and TGF- $\beta$ 1), proliferation and osteogenic differentiation of h-AdMSCs.

The curves of PDGF-AB and TGF- $\beta$ 1 release kinetics from aP-PRP/iC-HT-TPPs (Fig. 3) shows predominantly diffusive profiles, indicating no collapse of the scaffold structure at the time of the assays.

Controlled GFs release was achieved from aP-PRP-iC-HT-TPPs compared with aP-PRP alone. The maximum PDGF-AB release was obtained at 24 hours (Fig. 3A), whereas a concentration plateau was not observed for TGF- $\beta$ 1 at 72 hours (Fig. 3B).

In addition to the barrier of the structures, the interactions of GFs and scaffolds play an important role in the release. According to Hokugo et al. [35] and De Cock et al. [36], because GFs are generally basic proteins, in physiological conditions, they interact ionically with negatively charged surfaces.

In this work, we observed a higher delay in the PDGF-AB release of aP-PRP-iC-HT-TPPs mass ratio 2:1 compared with aP-PRP, suggesting electrostatic interactions with negative charges of the scaffold. At physiological pH, PDGF-AB bore a net positive charge (isoelectric point 9.8–10.5) [37].

For TGF- $\beta$ 1, a higher delay was observed for the scaffolds aP-PRP-iC-HT-TPPs at mass ratios of 5:1 and 10:1 compared with aP-PRP. Because TGF- $\beta$ 1 has the isoelectric point of 8.2, which is near the physiological pH (7.4), the positive charges

of the scaffolds had a smaller influence on delay [37].

In this case, we hypothesized that the delay was primarily due to the interaction of the negative fibrin network and the positive scaffold, which entrapped the GFs molecules.

Scanning electronic microscopy (Fig. 4) of aP-PRP showed a tangled network that was similar to the extracellular matrix. The microparticles were entrapped by the fibrin network, which provided an additional matrix for h-AdMSCs adherence and proliferation.

As assayed by MTT (Fig. 5A), the iC-HT-TPPs had a higher proliferation of h-AdMSCs compared with the positive control (PTC=DMEM with phenol 0.5%), which indicated not cytotoxicity.

The kinetic profiles (Fig. 5B) showed a long lag phase (~7 days) for aP-PRP-iC-HT-TPPs.

The proliferation of h-AdMSCs was lower than aP-PRP in the composite scaffolds at 2:1 and 5:1 mass ratios, whereas no proliferation was observed at 10:1.

Osteoblast differentiation is characterized by three stages: cell proliferation, matrix maturation, and matrix mineralization. During proliferation, several extracellular matrix proteins (procollagen I, TGF- $\beta$ , fibronectin) can be detected. The matrix maturation phase is characterized by maximal expression of ALP. Finally, at the beginning of matrix mineralization, genes for proteins such as osteocalcin, bone sialoprotein, and osteopontin are expressed and once mineralization is completed, calcium deposition can be visualized using adequate staining methods [38].

Significant ALP activity (Fig. 6) was obtained for aP-PRP-iC-HT-TPPs regardless of the mass ratio of CHT-TPP, indicating that osteogenic differentiation was stimulated.

In this work, ALP activity was determined in the culture medium and thus did not include the concentrations inside the gels. This may have also contributed to the lower values of ALP activities of the composite scaffolds compared with aP-PRP, due to the higher viscosity, which delayed the release of ALP.

In conclusion, we have demonstrated that the injectable composite scaffolds (aP-PRP-iC-HT-TPPs) promoted the controlled release of PDGF-AB and TGF- $\beta$ 1 from platelets primarily during the first 10 h. Although the physicochemical and rheological properties of iC-HT-TPPs increased the stability of the fibrin network, a significant proliferation of h-AdMSCs was observed only for the composite scaffold containing 2:1 chitosan-TPP. However, the osteogenic differentiation when evaluated by osteogenic marker ALP was stimulated in all mass ratios. Thus, the injectable composite scaffolds could be optimized to demonstrate their potential for regenerative medicine applications.

## Conflicts of Interest

The authors have no financial conflicts of interest.

## Ethical Statement

This study was approved by the Ethics Committee of the Medical Sciences School of the University of Campinas (UNI-CAMP; CAAE: 0972.0.146.000-11).

## REFERENCES

- Kretlow JD, Klouda L, Mikos AG. Injectable matrices and scaffolds for drug delivery in tissue engineering. *Adv Drug Deliv Rev* 2007;59:263-273.
- Hou Q, De Bank PA, Shakesheff KM. Injectable scaffolds for tissue regeneration. *J Mater Chem* 2004;14:1915-1923.
- Gutowska A, Jeong B, Jasionowski M. Injectable gels for tissue engineering. *Anat Rec* 2001;263:342-349.
- Costa-Pinto AR, Reis RL, Neves NM. Scaffolds based bone tissue engineering: the role of chitosan. *Tissue Eng Part B Rev* 2011;17:331-347.
- Berger J, Reist M, Mayer JM, Felt O, Peppas NA, Gurny R. Structure and interactions in covalently and ionically crosslinked chitosan hydrogels for biomedical applications. *Eur J Pharm Biopharm* 2004;57:19-34.
- Brack HP, Tirmizi SA, Risen Jr WM. A spectroscopic and viscometric study of the metal ion-induced gelation of the biopolymer chitosan. *Polymer* 1997;38:2351-2362.
- Hennink WE, van Nostrum CF. Novel crosslinking methods to design hydrogels. *Adv Drug Deliv Rev* 2002;54:13-36.
- Bhumkar DR, Pokharkar VB. Studies on effect of pH on cross-linking of chitosan with sodium tripolyphosphate: a technical note. *AAPS Pharm-SciTech* 2006;7:E50.
- Ibezim EC, Andrade CT, Marcia C, Barretto B, Odimegwu DC, de Lima FF. Ionically Cross-linked Chitosan/Tripolyphosphate Microparticles for the Controlled Delivery of Pyrimethamine. *Ibnosina J Med BS* 2011; 3:77-88.
- Harris R, Lecumberri E, Heras A. Chitosan-genipin microspheres for the controlled release of drugs: clarithromycin, tramadol and heparin. *Mar Drugs* 2010;8:1750-1762.
- Karnchanajindanun J, Srisa-ard M, Srihanam P, Baimark Y. Preparation and characterization of genipin-cross-linked chitosan microparticles by water-in-oil emulsion solvent diffusion method. *Natural Science* 2010; 2:1061-1065.
- Barnett Jr MD, Pomeroy GC. Use of platelet-rich plasma and bone marrow-derived mesenchymal stem cells in foot and ankle surgery. *Tech Foot Ankle Surg* 2007;6:89-94.
- Crane D, Everts PAM. Platelet Rich Plasma (PRP) Matrix Grafts. *Pract Pain Manag* 2008;8:12-26.
- Foster TE, Puskas BL, Mandelbaum BR, Gerhardt MB, Rodeo SA. Platelet-rich plasma: from basic science to clinical applications. *Am J Sports Med* 2009;37:2259-2272.
- Marx RE. Platelet-rich plasma: evidence to support its use. *J Oral Maxillofac Surg* 2004;62:489-496.
- Tabata Y. Tissue regeneration based on growth factor release. *Tissue Eng* 2003;9 Suppl 1:S5-S15.
- Shimojo AA, Perez AG, Galdames SE, Brissac IC, Santana MH. Performance of PRP associated with porous chitosan as a composite scaffold for regenerative medicine. *ScientificWorldJournal* 2015;2015:396131.
- Nasti A, Zaki NM, de Leonardi P, Ungphaiboon S, Sansongsak P, Rimoli MG, et al. Chitosan/TPP and chitosan/TPP-hyaluronic acid nanoparticles: systematic optimisation of the preparative process and preliminary biological evaluation. *Pharm Res* 2009;26:1918-1930.
- Flory PJ, Rehner Jr J. Statistical Mechanics of Cross-Linked Polymer Networks I. Rubberlike Elasticity. *J Chem Phys* 1943;11:512-520.
- Collins MN, Birkinshaw C. Investigation of the swelling behavior of crosslinked hyaluronic acid films and hydrogels produced using homogeneous reactions. *J Appl Polym Sci* 2008;109:923-931.
- Jin J, Song M. Chitosan and chitosan-PEO blend membranes cross-linked by genipin for drug release. *J Appl Polym Sci* 2006;102:436-444.
- Rädler JO, Koltover I, Jamieson A, Salditt T, Safinya CR. Structure and interfacial aspects of self-assembled cationic lipid-DNA gene carrier complexes. *Langmuir* 1998;14:4272-4283.
- Tan H, Chu CR, Payne KA, Marra KG. Injectable in situ forming biodegradable chitosan-hyaluronic acid based hydrogels for cartilage tissue engineering. *Biomaterials* 2009;30:2499-2506.
- Mosmann T. Rapid colorimetric assay for cellular growth and survival: application to proliferation and cytotoxicity assays. *J Immunol Methods* 1983;65:55-63.
- Gümüşderelioglu M, Aday S. Heparin-functionalized chitosan scaffolds for bone tissue engineering. *Carbohydr Res* 2011;346:606-613.
- Perez AG, Lichy R, Lana JE, Rodrigues AA, Luzo AC, Belangero WD, et al. Prediction and modulation of platelet recovery by discontinuous centrifugation of whole blood for the preparation of pure platelet-rich plasma. *Biores Open Access* 2013;2:307-314.
- Mi FL, Shyu SS, Lee ST, Wong TB. Kinetic study of chitosan-tripolyphosphate complex reaction and acid-resistive properties of the chitosan-tripolyphosphate gel beads prepared by in-liquid curing method. *J Polym Sci Pol Phys* 1999;37:1551-1564.
- Kablík J, Monheit GD, Yu L, Chang G, Gershkovich J. Comparative physical properties of hyaluronic acid dermal fillers. *Dermatol Surg* 2009;35 Suppl 1:302-312.
- Ikeda S, Nishinari K. "Weak gel"-type rheological properties of aqueous dispersions of nonaggregated kappa-carrageenan helices. *J Agric Food Chem* 2001;49:4436-4441.
- Clark AH, Ross-Murphy SB. Structural and mechanical properties of biopolymer gels. *Adv Polym Sci* 1987;83:57-192.
- de Melo F, Marijnissen-Hofsté J. Investigation of physical properties of a polycaprolactone dermal filler when mixed with lidocaine and lidocaine/epinephrine. *Dermatol Ther (Heidelb)* 2012;2:13.
- Ohrlund A, Edsman K, Stureson C, Nord L, Helander Kenne A, Nasstrom J. Lifting capacity of hyaluronic acid (HA) dermal fillers. Presented at: 8th Anti-Aging Medicine World Congress & MeiSpa (AMWC); 2010 Apr 8-10; Monte-Carlo, Monaco.
- Bentkover SH. The biology of facial fillers. *Facial Plast Surg* 2009;25:73-85.
- Peppas NA, Sahlin JJ. Hydrogels as mucoadhesive and bioadhesive materials: a review. *Biomaterials* 1996;17:1553-1561.
- Hokugo A, Ozeki M, Kawakami O, Sugimoto K, Mushimoto K, Morita S, et al. Augmented bone regeneration activity of platelet-rich plasma by biodegradable gelatin hydrogel. *Tissue Eng* 2005;11:1224-1233.
- De Cock LJ, De Wever O, Hammad H, Lambrecht BN, Vanderleyden E, Dubrue P, et al. Engineered 3D microporous gelatin scaffolds to study cell migration. *Chem Commun (Camb)* 2012;48:3512-3514.
- Wang C, Li J, Yao F. Application of Chitosan-Based Biomaterials in Tissue Engineering. In: Yuji Y, editor. *Chitosan-Based Hydrogels: Functions and Applications*. New York: CRC Press; 2011. p.424.
- Stein GS, Lian JB. Molecular mechanisms mediating developmental and hormone-regulated expression of genes in osteoblasts: an integrated relationship of cell growth and differentiation. In: Noda M, editor. *Cellular and molecular biology of bone*. Tokyo: Academic Press; 1993. p.47-95.